Real-Time imaging with a high speed X-Ray CT system

Thompson, William M and Lionheart, William RB and Morton, Edward J

2012

MIMS EPrint: **2012.36**

Manchester Institute for Mathematical Sciences
School of Mathematics

The University of Manchester

Reports available from: http://eprints.maths.manchester.ac.uk/
And by contacting: The MIMS Secretary
School of Mathematics
The University of Manchester
Manchester, M13 9PL, UK

ISSN 1749-9097

Real-Time imaging with a high speed X-Ray CT system

William M. Thompson[1], William R. B. Lionheart[1], Edward J. Morton[2]

1. University of Manchester, 2. Rapiscan Systems

ABSTRACT

The Real Time Tomography (RTT) system is a new type of fast cone beam CT scanner, using fixed rings of multiple sources and detectors in an offset geometry. We demonstrate the potential of this system for use in the imaging of high speed dynamic processes, such as moving fluid flows. The effect of the source firing pattern is discussed, with application to increasing the temporal resolution of the system. Through the use of a simple temporal regularisation term, we show that temporal resolution can be further increased, at the expense of a slight loss in spatial resolution.

Keywords X-ray CT, cone beam, dynamic imaging, real-time imaging

1 INTRODUCTION

Conventionally, X-ray tomographic imaging systems have used a single X-ray source and an array of detectors which together rotate around the object of interest to form a set of X-ray projections through the object. These projections can be reconstructed to form an image of the object in 2D or 3D, depending on whether the detector configuration is single row fan beam or multi-row cone beam.

Due to the mechanical motion involved in this scanning process, scan rates are restricted to only a few source revolutions per second. The latest dual source medical CT scanners are able to perform just over 3 per second (Krauss et al. 2011); this gives a reconstructed image frame rate of less than 10 per second. In some applications, such frame rates are too slow to provide the required temporal resolution; for example in the visualisation of the flow of liquids in pipes.

The main factor limiting the speed of conventional rotating gantry cone beam CT scanners is the physical rotation of the source (Kalender, 2006). To address this problem, it is necessary to eliminate the mechanical scanning motion, replacing this with an electronic equivalent comprising a circular array of X-ray sources which can be selected individually under computer control. Through the choice of a suitable source scanning sequence, the impression of movement can be generated without physical motion of any component of the system.

A Real-Time Tomography (RTT) system has been developed to solve this technological problem (Morton et al. 1999, Morton, 2006), in which an approximately circular array of X-ray sources over an angular distribution of 180 degrees plus fan angle is matched with a corresponding array of X-ray detectors to provide a no-moving-parts X-ray tomographic scanning system. The plane containing the X-ray sources is offset from the plane containing the X-ray detectors to avoid attenuation of the primary beam before it is transmitted through the object under inspection.

The X-ray sources comprise an array of electron guns, each of which is controlled by an independent electronic switching circuit. These switching circuits can be pulsed in microsecond timescales. The electron beam from a given source is accelerated through a high potential difference to a tungsten coated anode to produce X-rays. A single distributed anode is arranged in a circular arrangement such that each electron gun irradiates a different region of the anode around the circumference of a circle or polygon, each resulting in an effective X-ray focus when viewed from the detectors of typically 1mm^2. The electron gun control electronics can be programmed to irradiate the electron guns in any given sequence. Therefore, this is a flexible data acquisition platform and is capable of generating tomographic scan data at theoretical source rotation rates of up to 480 frames per second.

2 THE RTT20 SYSTEM

RTT20 is a small-scale prototype RTT system which has been acquired by the University of Manchester, where it is expected to be used for imaging moving fluid and granular flows in order to provide experimental validation of mathematical models. A two-dimensional cross-section of the RTT20 geometry is shown in figure 1; the sources are arranged in 8 blocks of 32, with two “missing” blocks of sources at the bottom, creating an incomplete source ring. The incomplete ring is part of the original design to enable a small

scanner to be easily fixed onto pipes for imaging flowing fluids. The two blocks adjacent to the gap also do not use their outermost 4 sources, giving a total of 248 sources. There is one full ring of detectors arranged in 21 blocks of 16, giving 336 detectors in total; this is offset from the source plane by 5.48mm in the *z* direction. The tunnel diameter is 20cm (hence RTT20) giving the reconstruction region of interest (ROI) as a circle of diameter 200mm.

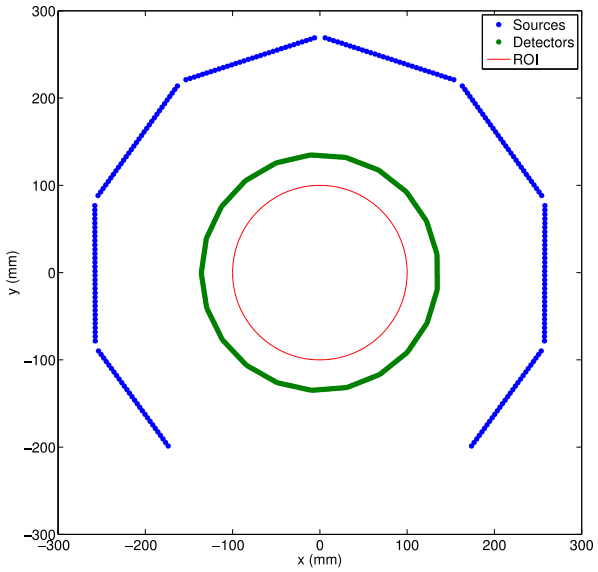

Figure 1: The RTT20 geometry

The machine is capable of acquiring a complete set of projections from all 248 sources 60 times per second, enabling imaging of very fast moving processes; a complete set of projections is known as a *revolution*. Sources may be fired in almost any order we desire; for a general RTT system with *N* sources, this is defined by a bijective function

$$\phi: [1, N] \longrightarrow [1, N], \tag{1}$$

known as a *firing order*. The firing order used for collection of the RTT20 experimental data is defined for 256 sources by the function

$$\phi(i) = \left\{\left(32(i-1) + \left\lfloor \frac{i-1}{8} \right\rfloor\right) \bmod 256\right\} + 1, \tag{2}$$

where$\lfloor . \rfloor$ denotes the round towards negative infinity operator. The first and last 4 sources in the sequence are simply removed to reduce this to 248 sources.

3 THE RECONSTRUCTION PROCESS

The reconstruction of an RTT20 dynamic data set forms a sequence of images, each of which is referred to as a *frame*. The simplest method of reconstruction is to regard each revolution as representing a frame and reconstruct each one of these independently. For applications where the motion of the object is slow compared to the data collection rate this should be adequate. However, if the firing order is chosen appropriately, so that the distribution of projection angles is even for smaller subsets of projections, then we may divide each revolution's full set of projections to represent multiple frames, effectively trading spatial for temporal resolution. The firing order described by equation (2) satisfies this condition reasonably well but is not optimal.

The process of reconstructing each two-dimensional frame is simple and well understood; however, the construction of RTT20 presents some problems. Firstly, the polygonal nature of the source and detector rings means that the distribution of projection angles, and the angles of rays within each projection, are highly uneven. This, combined with the incomplete source ring, causes an uneven sampling of the two-dimensional Radon transform; this is shown in figure 2.

Secondly, the offset detector means that we do not really measure rays in a plane through the object. However, compared to the *x-y* resolution of the system, the effect of the offset is considered small enough to ignore within the reconstruction region of interest.

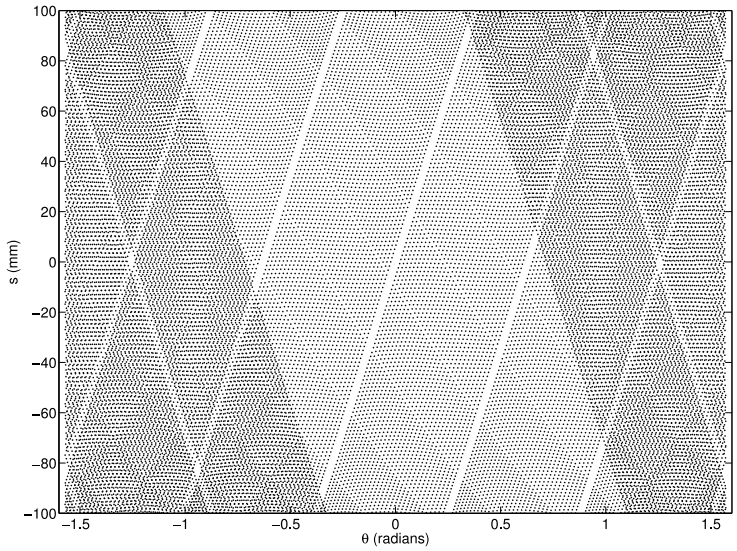

Figure 2: Distribution of sampling points in the 2D Radon transform domain

4 FIRING ORDER CONSIDERATIONS

The choice of firing order is subject to restrictions as follows; firstly, it must be defined as a sequence of length equal to the number of sources by a suitable function as in (1). Sequences of arbitrary length are not permitted. Secondly, due to thermal load on the sources, for every set of three consecutive projections, sources from three separate source blocks must be used. In particular, this prohibits the use of the sequential firing order which gives rise to the classical circular source trajectory.

The goal when considering the choice of firing order for imaging dynamic processes using an RTT system is to optimise the spread of projection angles for the projections representing each frame. Due to the first restriction on the firing order, the number of frames per revolution must be an integer; hence the number of projections representing each frame must be a divisor of the total number of sources.

For RTT20 with 248 sources, the prime factors of 248 are 2, 2, 2 and 31; hence possible choices for the number of frames per revolution, and therefore also projections per frame, are 1, 2, 4, 8, 31, 62, 124 and 248. Letting f_s represent the number of frames per revolution, a simple way to optimise the firing order is to define it by the function

$$\phi(i) = \left\{\left(f_s(i-1) + \left\lfloor \frac{f_s(i-1)}{248} \right\rfloor\right) \bmod 248\right\} + 1. \tag{3}$$

Of course, for certain values of f_s, this will violate the second firing order restriction. However, this violation is easily avoided by using a permutation of the source numbers for each frame's projections. This gives a firing order of the form

$$\phi(i) = \left\{\left(k f_s(i-1) + \left\lfloor \frac{f_s(i-1)}{248} \right\rfloor\right) \bmod 248\right\} + 1, \tag{4}$$

where*k* is some integer coprime to the number of projections per frame.

5 RECONSTRUCTION ALGORITHMS

5.1 Analytical Algorithms

Analytical reconstruction algorithms based on filtered back projection (FBP) for the 2D fan beam geometry are well known (Kak and Slaney, 1988). However, these assume an equal spacing of the projection angles, and either an equiangular or equally spaced linear sampling scheme for the rays within each projection. Due to the construction of RTT20, with its polygonal source and detector rings, neither of these conditions are satisfied. For applications where low reconstruction time is important, such as real time observation of flow through an oil pipe for example, taking all 248 projections per frame and using a simple interpolation to the

parallel beam geometry gives adequate results. However, for fast moving objects, motion artefacts will be observed.

5.2 Algebraic Reconstruction

For applications where the data acquisition and image analysis processes are separate, such as the scientific applications the machine will be used for at the university, the problem is small enough to enable solution by algebraic methods in a reasonable amount of time. Algebraic methods make no assumptions at all about the system geometry, so in theory should be capable of improved reconstructed image quality. Performance of algebraic algorithms with reduced numbers of projections is also better, which should allow fewer projections per frame, resulting in better temporal resolution.

We let the matrix *A* represent the projection process for each complete set of 248 projections; this may represent more than one frame, and is simply re-used for each revolution. Elements of *A* are calculated using the ray tracing algorithm of Jacobs et al. (1998), which is itself a development of Siddon's algorithm (Siddon, 1985). In order to take the offset geometry into account, ray tracing is performed in 3D; to ensure only a single slice is considered, the voxels are simply defined to be long in the *z* direction. This has been implemented in MATLAB as a C `.mex` routine, with output in the MATLAB double precision sparse matrix format. Using 1×1 mm pixels and covering the entire circular ROI, storage requirements for *A* are approximately 100MB.

For each revolution, the system of equations $Ax = b$is solved using the conjugate gradient least squares (CGLS) algorithm. We use the MATLAB implementation of CGLS provided in Hansen's Regularisation Tools package (Hansen, 1998).

5.3 Regularisation

Although with CGLS, the number of iterations plays the role of a regularisation parameter, it is unclear how many iterations should be performed in order to provide the correct degree of regularisation. We may therefore apply additional systematic regularisation by solving the augmented system

$$\begin{bmatrix} A \\ \alpha L \end{bmatrix} x = \begin{bmatrix} b \\ 0 \end{bmatrix}, \tag{5}$$

in the least squares sense, where α is a regularisation parameter, *L* is some finite difference approximation to a differential operator, for example the Laplacian, and 0 is the zero vector of length equal to the total number of image pixels. This gives the least squares solution

$$\arg\min_{x}\{\|Ax - b\|_2^2 + \alpha^2 \|Lx\|_2^2\}, \tag{6}$$

In addition to providing regularisation in the spatial dimensions, by considering the data set as a whole, rather than as a set of discrete independent frames, we can also add regularisation in the temporal dimension. The matrix A_{total}, representing the whole system, is formed from *A* by a Kronecker product with the identity matrix of size equal to the number of revolutions.
Regularisation has been performed by taking *L* to be the three-dimensional discrete Laplacian. By incorporating the regularisation parameter into the matrix *L*, it is possible to choose differing amounts of regularisation in the spatial and temporal dimensions. Letting *m* and *n* be the number of image pixels in the *x* and *y* directions respectively, and letting *p* be the number of frames, *L* has the following Kronecker product decomposition:

$$L = \alpha_s I_p \otimes I_n \otimes D_m + \alpha_s I_p \otimes D_n \otimes I_m + \alpha_t D_p \otimes I_n \otimes I_m, \tag{7}$$

whereI_m is the $m \times m$ identity matrix, D_m is the one-dimensional discrete Laplacian on *m* points and α_s and α_t are respectively the spatial and temporal regularisation parameters.

6 RESULTS

6.1 Simulated Data (Original Firing Order)

Simulated data were generated for a ball of radius 10mm, moving horizontally along a line through the centre of the scanner in a sinusoidal motion of frequency 0.5Hz and amplitude 80mm. Ray integrals were calculated analytically, with the object position being re-calculated for each projection. The simulation was performed at

the scanner's standard speed of 60 revolutions per second, and using the firing order described by equation (2). 1% Gaussian noise was added to the calculated data.

Figure 3 shows a frame from reconstructions of the simulated data using differing values of the temporal regularisation parameter, comparing a full set of projection data per frame with 31 projections per frame (8 frames per revolution). In all cases, the spatial regularisation parameter was chosen empirically as $\alpha_s = 5$. Figures 4 and 5 show respectively the 2-norms of the data error, and the error from the reference image at each iteration.

We see that by reducing the number of projections per frame, the motion between subsequent frames is reduced so that it makes sense to smooth in the temporal dimension. By doing this, streak artefacts are reduced and temporal resolution has increased by a factor of 8.

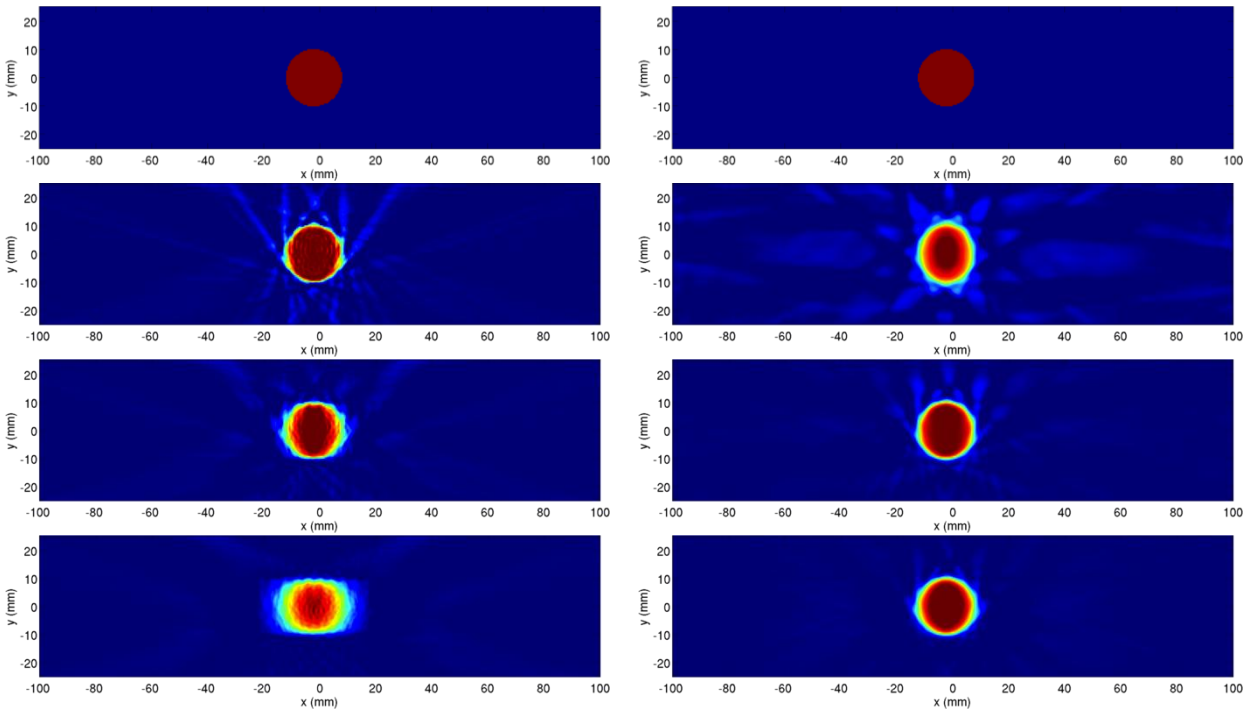

Figure 3: Reconstructed images of a single frame from the simulated data using the original firing order (left, 248 projections; right, 31 projections; top – bottom, reference image, $\alpha_t = 0$, $\alpha_t = 5$, $\alpha_t = 25$)

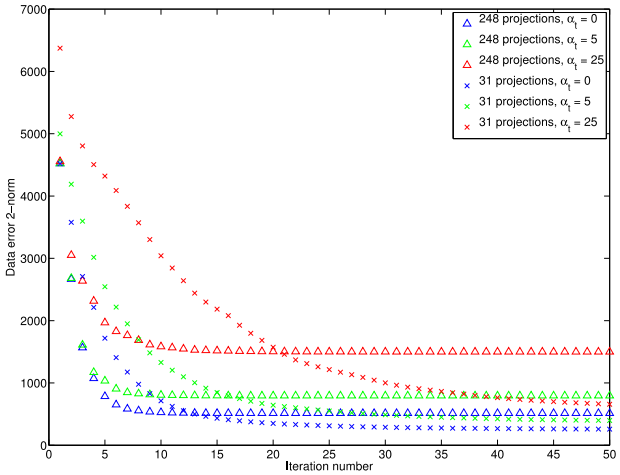

Figure 4: Data error for the simulated data reconstructions using original firing order

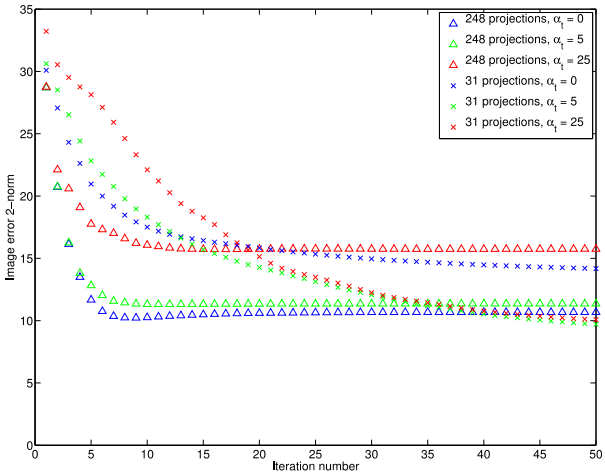

Figure 5: Image error for the simulated data reconstructions using original firing order

6.2 Simulated Data (Optimised Firing Order)

The simulated data experiment from section (6.1) was repeated using a firing order of the form given in equation (4), with $f_s = k = 8$, giving 31 projections per frame as before. As a more extreme test, this was

compared against the firing order with parameters$f_s = 31$ and$k = 3$, giving 8 projections per frame; due to the prime factors of 248, no intermediate choices are possible.

Reconstructions of a single frame using these firing orders are compared for differing values of the temporal regularisation parameter in figure 6. As before, the spatial regularisation parameter was chosen empirically as $\alpha_s = 5$. Figures 7 and 8 show respectively the 2-norms of the data error, and the error from the reference image at each iteration.

Results with 31 projections per frame show that optimising the firing order gives substantially improved image quality. Using a small amount of temporal regularisation yields slightly lower reconstructed image error. Using 8 projections per frame predictably shows drastically reduced image quality; however, there may be applications where the increased temporal resolution may be more important.

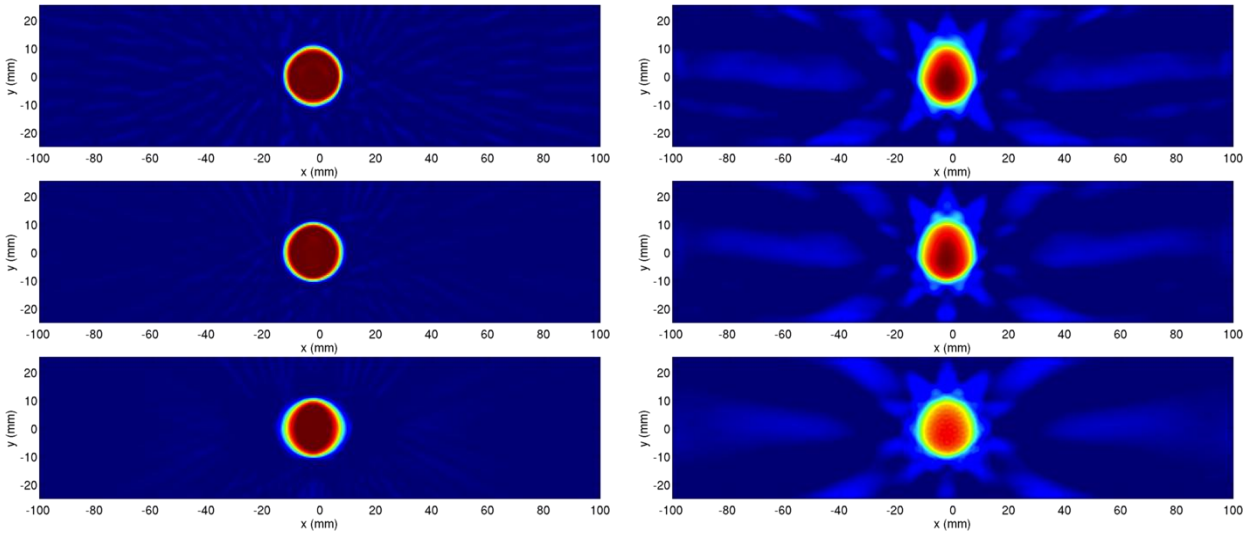

Figure 6: Reconstructed images of a single frame from the simulated data using optimised firing orders (left, 31 projections; right, 8 projections; top – bottom, $\alpha_t = 0$, $\alpha_t = 5$, $\alpha_t = 25$)

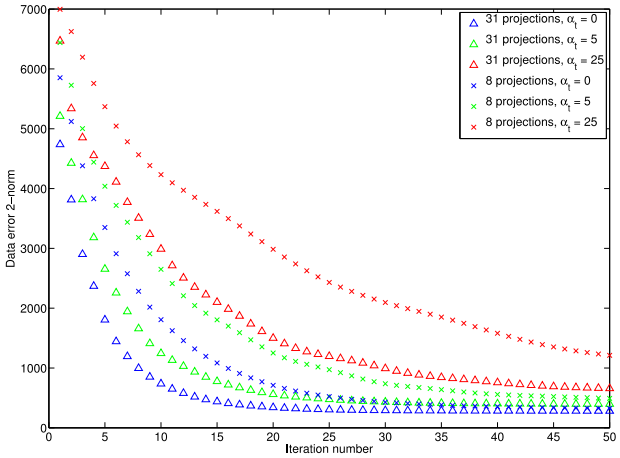

Figure 7: Data error for the simulated data reconstructions using optimised firing order

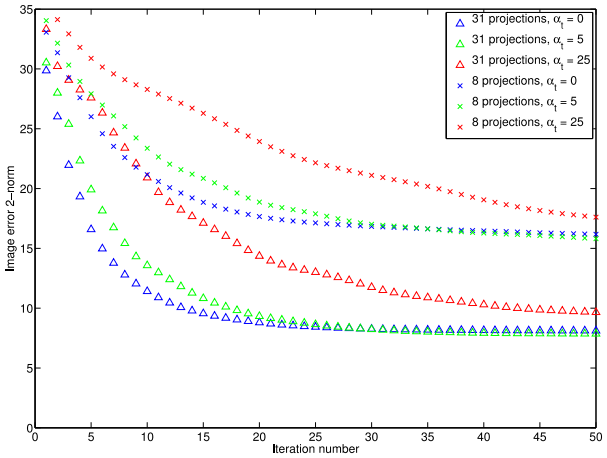

Figure 8: Image error for the simulated data reconstructions using optimised firing order

6.3 Real Data

Real experimental data were available for a mixture of oil, water and air moving in a bottle. The data set consists of 61 revolutions representing 1 second of the motion, and was collected during the machine's initial testing process. The scanner settings used were a voltage of 120keV, and current of 10mA. Three of the sources in the prototype scanner were defective, resulting in a total of 245 sources being used.

Figure 9 shows a frame from reconstructions of the data, again using differing values of the temporal regularisation parameter, comparing a full set of projection data per frame with 49 projections per frame (5 frames per revolution). Again, in all cases, the spatial regularisation parameter was chosen empirically as$\alpha_s = 5$. Figure 10 shows the 2-norm of the data error at each iteration.

The motion in this case is not as fast as the simulated data, and reasonable results are obtained by simply using all 245 projections per frame. However, by using only 49 projections per frame and applying temporal regularisation, temporal resolution has increased by a factor of 5; this improvement is very noticeable when viewing the full dynamic reconstruction as a movie. Although the 49 projection temporally regularised images are noticeably softer than those using the full set of projections per frame, they compare well. It is likely that further improvement could be achieved through the use of an optimised firing order, though we do not currently have experimental data available to confirm this.

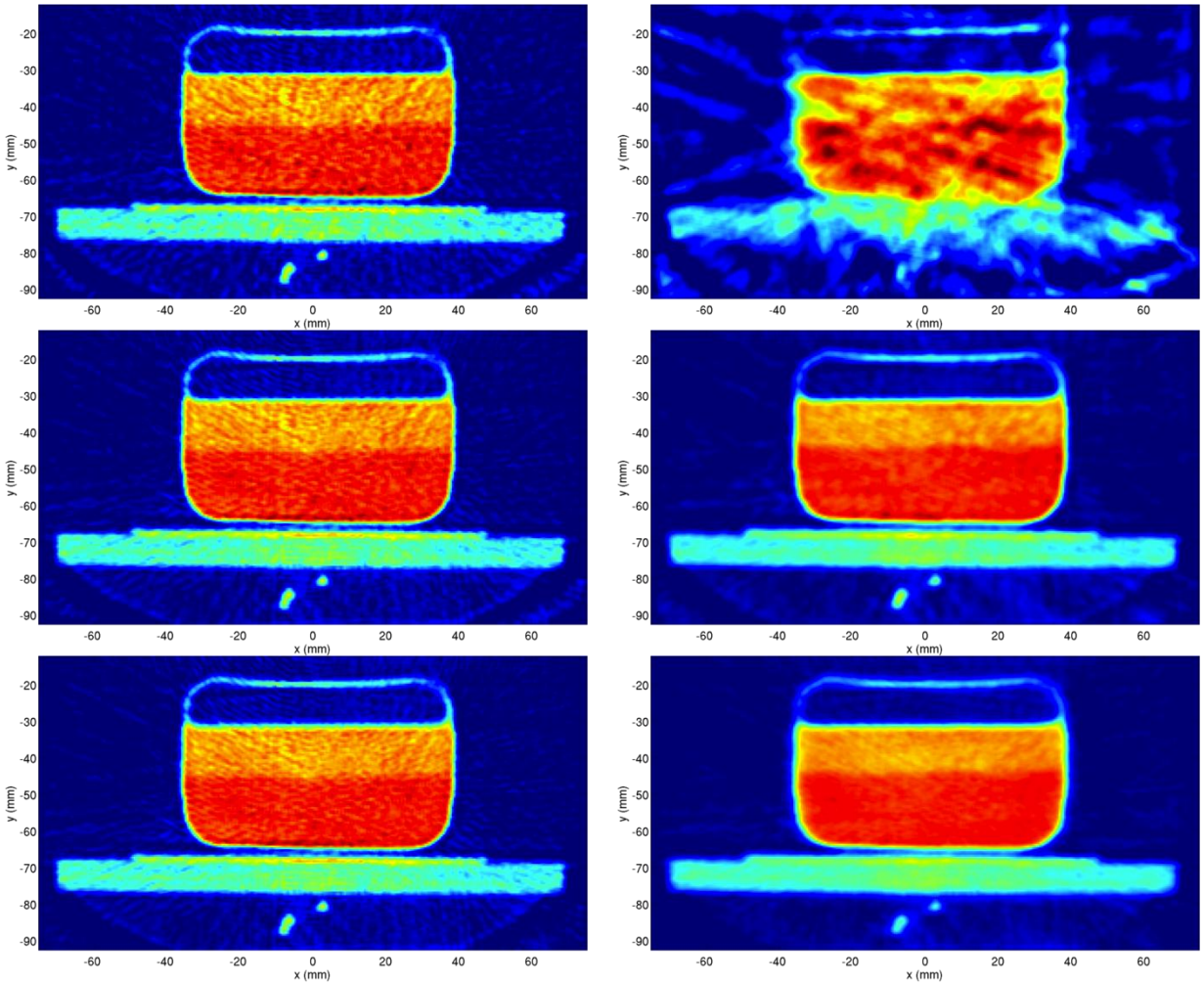

Figure 9: Reconstructed images of a single frame from the oil and water data (left, 245 projections; right, 49 projections; top – bottom, $\alpha_t = 0$, $\alpha_t = 5$, $\alpha_t = 25$)

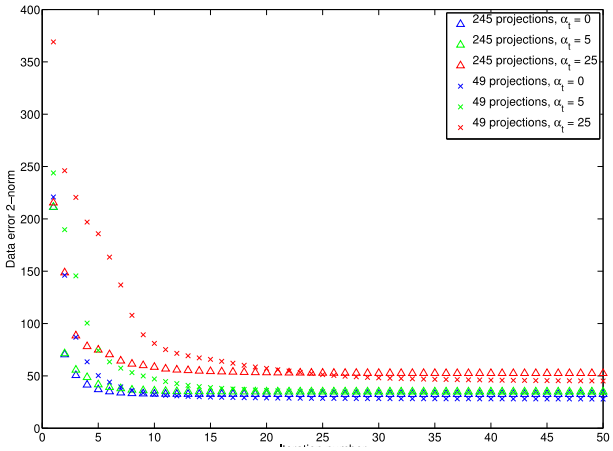

Figure 10: Data error for the oil and water data reconstructions

7 CONCLUSIONS

The RTT system has the potential to produce some novel visualisations of rapidly moving processes such as fluid and granular flows. Problems caused by the highly uneven sampling generated by the RTT20 geometry have been solved by using algebraic reconstruction and regularisation, rather than the more widely used filtered back projection based algorithms. Through the use of optimised source firing patterns, combined with a simple temporal regularisation process, it is shown that image quality can be maintained whilst using fewer projections per frame. It has been demonstrated that temporal resolution can be increased in real world applications by at least a factor of 5, with only minor impact on reconstructed image quality.

8 ACKNOWLEDGEMENTS

The authors would like to thank Rapiscan Systems and EPSRC (grant EP/E010997/1) for supporting this work. We would particularly like to thank the RTT development team for providing us with access to technical details of the system and experimental data.

9 REFERENCES

KRAUSS B., SCHMIDT B., FLOHR T.G., (2011), Dual source CT, in JOHNSON T., FINK C., SCHONBERG S.O., REISER M.F., (eds.) *Dual energy CT in clinical practice, ser. Medical Radiology,* Springer Berlin Heidelberg, pp. 11-20.

KALENDER W.A., (2006), X-ray computed tomography, *Phys. Med. Biol.*, vol. 51, no. 13, p. R29.

MORTON E.J., LUGGAR R.D., KEY M.J., KUNDU A., TAVORA L.M.N., GILBOY W.B., (1999) Development of a high speed x-ray tomography system for multiphase flow imaging, *IEEE Trans. Nucl. Sci.*, vol. 46 III(1), pp. 380-384.

MORTON E.J., (2006), X-ray monitoring, *US patent application US2006023961(A1).*

KAK A., SLANEY M., (1988), *Principles of computerized tomographic imaging*, IEEE Service Center, Piscataway, NJ.

JACOBS F., SUNDERMANN E., DE SUTTER B., LEMAHIEU I., (1998), A fast algorithm to calculate the exact radiological path through a pixel or voxel space, *J. Comput. Inform. Technol.*, vol. 6, pp. 89-94.

SIDDON R.L., (1985), Fast calculation of the exact radiological path for a 3-dimensional CT array, *Med. Phys.*, vol. 12, no. 2, pp. 252-255.

HANSEN P.C., (1998), Regularization tools – a MATLAB package for analysis and solution of discrete ill-posed problems – version 3.0 for MATLAB 5.2, *Numer. Algorithms*, vol. 6, pp. 1-35.